

MAXIMUM ENTROPY IMAGING AND
SPECTRAL DECONVOLUTION FOR COMPTEL

A.W. Strong¹, P. Cabeza-Orcel^{4*}, K. Bennett⁴, W. Collmar¹, R. Diehl¹,
J.W. den Herder², W. Hermsen², G. Lichti¹, M. McConnell³, J. Ryan³,
H. Steinle¹, V. Schönfelder¹, C. Winkler⁴

1. Max-Planck-Institut für Extraterrestrische Physik, Garching, FRG
2. Laboratory for Space Research, Leiden, The Netherlands
3. University of New Hampshire, Durham N.H., USA
4. Space Science Dept. of ESA, ESTEC, Noordwijk, The Netherlands

ABSTRACT

The method of maximum entropy will be used to generate sky maps from COMPTEL flight data. The application to COMPTEL allows the full instrument response to be included, and extensive tests with calibration data give encouraging results. The sensitivity of the method to background has been investigated. Maximum entropy will also be used for deconvolution of burst and solar energy spectra. Successful tests have been made with calibration and also SMM solar flare data.

1. IMAGING OF COMPTON TELESCOPE DATA

The generation of images from Compton telescope data presents an interesting challenge and one which is timely in view of the COMPTEL instrument on GRO. Application of the Maximum Entropy method (MEM) to γ -ray astronomy was first described by Skilling et al. (1979) for COS-B spark chamber data; Diehl and Strong (1987) discussed both COS-B and COMPTEL applications, and Strong et al. (1990) made simulations of multiple source imaging with the COMPTEL response. Varendorff (1991) has applied MEM to balloon observations of the Galactic centre region with the MPE Compton telescope with excellent results.

The Compton telescope is *a priori* an excellent candidate for MEM, not only because no other method has proved able to provide sky maps in the strict sense of intensity distributions consistent with the data (other methods give various types of probability distributions which cannot be interpreted as intensities), but also because of the nature of the instrumental data (see Schönfelder et al., these proceedings, for a description of the instruments and

* present address: Les Edition Belins, Pour La Science, Paris, France

its measurement principles). The data is characterized by a 3D point-spread-function (PSF) with the additional dimension (after the two spatial ones) being provided by the Compton scatter angle. The 'data space' is similarly 3D (or more if energy resolution is included). Since we want to generate 2D skymaps it is clear that our 'data space' is very different from our 'image space'. This is just the kind of problem where MEM is effective; in fact the more different the data and image spaces are the more useful are the so-called 'indirect imaging' methods. In this sense we are nearer to radio interferometry or Fourier spectroscopy where indirect imaging is the natural technique. One interesting aspect of Compton telescope data is that the Compton scatter 'dimension' gives an 'overdetermination' of the image; it is as if we observed the sky with many separate 2D PSFs and attempt to use them all simultaneously for the reconstruction. One advantage of having very different image and data spaces and of overdetermination is that unwanted correlations between image and data (e.g. the image following point-to-point statistical variations in the data) are practically eliminated.

2. APPLICATION OF MAXIMUM ENTROPY TO COMPTEL IMAGING

Maximum entropy is a general technique for deconvolution which produces the 'flattest' solution consistent with the given data and response function. Only features for which there is 'evidence' in the data are thereby obtained; at least this is the main property claimed by the advocates of MEM. The principles of the method are described in the literature (e.g. Gull and Skilling 1984), and will not be repeated here. The software package used is MEMSYS2 from Maximum Entropy Data Consultants Ltd of Cambridge, England. The user provides a function (see below) which computes the data space response to any given input image; the package then allows an iterative solution for the maximum entropy image starting from a uniform (or reference) image and iterating towards improving the fit to the data. A particular version of the software allows the correct treatment of data containing small or zero data values; the log-likelihood function for Poisson statistics is then used instead of the χ^2 adopted in the standard version. This is particularly important since we want to use binsizes small enough to exploit the instrumental angular resolution and this may well imply small statistics per bin.

The COMPTEL image space is defined in a coordinate system (χ_o, ψ_o) analogous to longitude and latitude but quite generally oriented. The COMPTEL data space is defined as $(\chi, \psi, \bar{\varphi})$ where χ, ψ are angles defining the direction of the photon after scattering in the upper (D1) detector layer (using the same coordinate system as (χ_o, ψ_o)) and $\bar{\varphi}$ is the Compton scatter angle computed from the energy deposits in the upper and lower detectors. The full response of the instrument to a given input image is complicated but a representation which is reasonably fast to compute and which preserves all the essential features is:

$$n(\chi, \psi, \bar{\varphi}) = g(\chi, \psi) d\Omega t \int_{\chi_o} \int_{\psi_o} I(\chi_o, \psi_o) A(\chi_o, \psi_o) f(\phi_g(\chi, \psi, \chi_o, \psi_o), \bar{\varphi}) d\chi_o d\psi_o \quad (1)$$

where $n(\chi, \psi, \bar{\varphi})$ is the expected count in a dataspace cell, $g(\chi, \psi)$ is the probability that a photon scattered in D1 into a direction (χ, ψ) encounters a D2 module (a purely geometrical effect which reflects the fact that the D1 and D2 layers consist of discrete modules), $I(\chi_o, \psi_o)$ is the image space intensity distribution, $A(\chi_o, \psi_o)$ is the area of the exposed D1 surface (about 4.2 m²), $f(\phi_g(\chi, \psi, \chi_o, \psi_o), \bar{\varphi})$ is the probability that a photon encountering D1 makes an interaction in both D1 and D2, scatters through an angle ϕ_g and has a measured Compton scatter angle of $\bar{\varphi}$. It is defined for a 'infinite' extent of the D2 layer, since the discrete nature of D2 is included in 'g'. It includes among other things the energy-dependent interaction probability in D1 (not therefore included in A) and the effects of incomplete absorption in D2. $d\Omega$ is the solid angle covered by the bin at (χ, ψ) , t is the exposure time. $f(\phi_g, \bar{\varphi})$ is referred to here as the 'PSF' since it has the property of being

(almost) independent of the input direction of the photon and here is similar to the normal type of PSF encountered in optics. This is achieved by the definition in terms of an infinite D2 layer and the removal of the geometrical part of the response from the convolution. If this were not done then every point in image space would have a different 'PSF' and the computational requirement would be much too large.

Note that the PSF would be a perfect cone defined by $\phi_g = \bar{\varphi}$ if the energy and position determinations in D1 and D2 were exact. The finite energy and position resolutions lead to a widening of the cone; in particular there is a filling in of regions with $\bar{\varphi} < \phi_g$ due to incomplete absorption in D2 (see Diehl et al., these proceedings).

The response representation given by equation(1) enables a fast computation of the response to any given input image provided the convolution with the PSF can be computed fast; in practice we have used an FFT method (in particular: Winograd FFT which is not restricted to powers of two) which treats the spherical coordinate system as a locally flat Cartesian system. Unfortunately this approximation is increasingly poor as we go to larger scatter angles (characteristic of lower photon energies); but explicit 'brute force' computation of the convolution is at present ruled out as it involves very large computer resources. A fast method for convolving a function on the sphere, if it exists, appears not to be generally known; in the long term, it may be necessary to use 'brute force' with vector processors. However the FFT method is good enough when the scatter angle is not too large, as the practical results below bear out.

For clarity I have omitted the energy dependence of terms in equation (1); however it should be clear that in a real application an additional convolution over the input intensity spectrum is required, and that the PSF is an energy-dependent function. Methods for obtaining the PSF from calibration data are discussed by Diehl et al. (these proceedings).

3. RESULTS USING CALIBRATION SOURCES

The calibration of COMPTEL included sources with energies from 0.83 to 20 MeV. These data can be used as a test of the MEM deconvolution, although the finite distance of the source (about 8m) means some spreading of the image. This can be minimized by using data from only one D1 detector; the spread is then about 2° . This problem does not of course arise in flight. Since the sources used were quite strong the signal-to-background ratio is not typical of flight situations, so it is necessary to add in data from background runs to obtain more realistic tests. Data for different source positions can be combined to simulate more than one source in the field-of-view and test the spatial resolution for source separation as a function of signal-to-background.

We concentrate on one source energy, 6.1 MeV and a configuration of 3 sources separated by 10° , and 2 sources separated by 5° . The source counts are typical of what might be expected for a Crab-like source and a COMPTEL observation of 2 weeks. Table 1 summarizes the cases presented here.

For the ideal case of no added background (Fig 3.1) the sources are completely resolved and in the correct positions, with no artefacts; this establishes the basic correct operation of the method.

If the background is increased to 5 times the counts for one source (Fig 3.2) the sources are still well imaged but the contrast is smaller. Edge effects become noticeable: some parts of the image near the edge of the field are not constrained by the data and are assigned the 'default' value defined by the user.

Further increase of the background to 16 times the counts for one source (Fig 3.3) reduces the source visibility and contrast is further reduced. Some extra features appear; however it should be noted that the 'background' data used consists of runs where sources in

Table 1. data used for maximum entropy images of calibration sources

Figure	Source energy	Source configuration Angles from axis	Counts per source	Total counts
3.1	6.1 MeV	0°, 10°, 20°	1470	4424
3.2		0°, 10°, 20°	1470	12408
3.3		0°, 10°, 20°	1470	28367
3.4		0°, 5°	1470	3480
3.5		0°, 10°, 20°	1470	12408

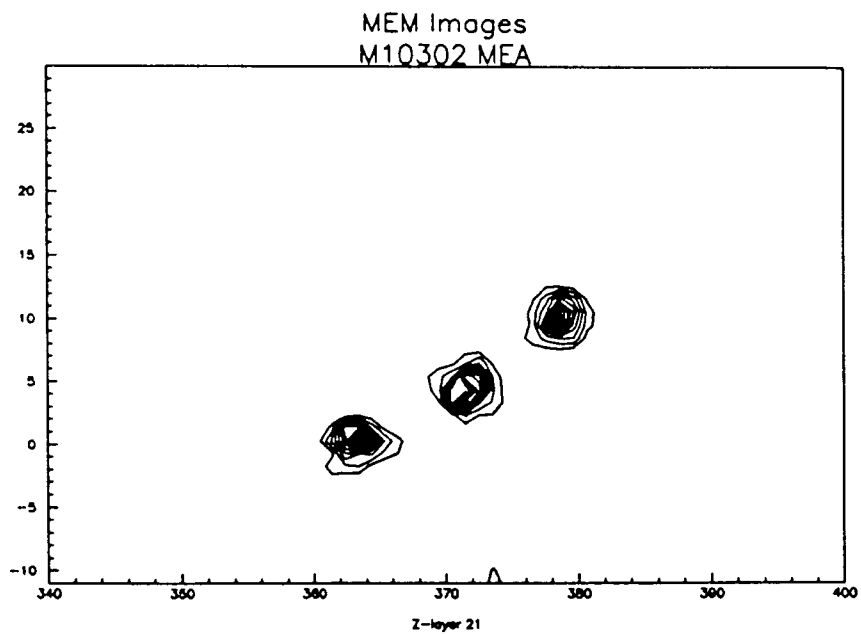


Fig 3.1. MEM images of three 6.1 MeV calibration sources separated by 10°, without added background. Details in Table 1.

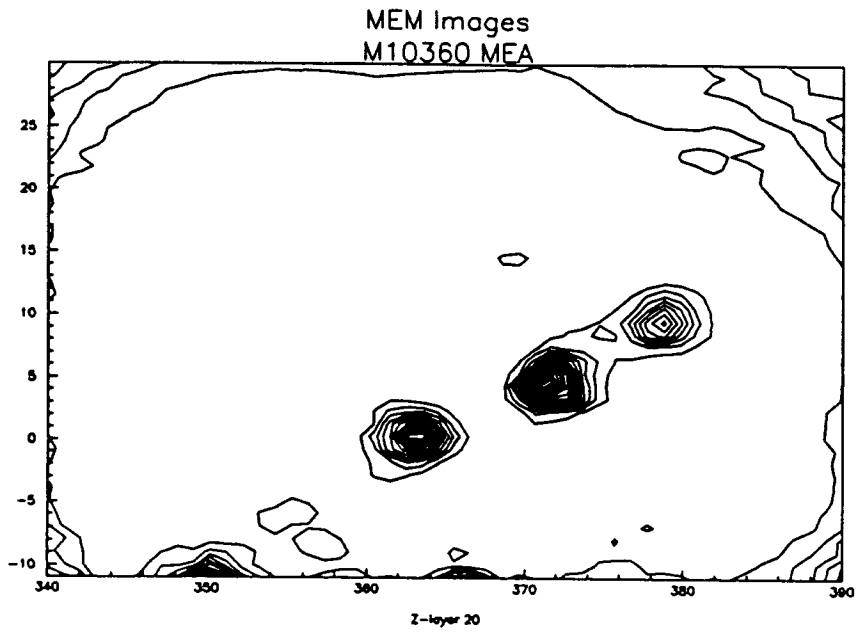


Fig 3.2. Adding a significant amount of background reduces the quality of the image, but the sources are clearly visible.

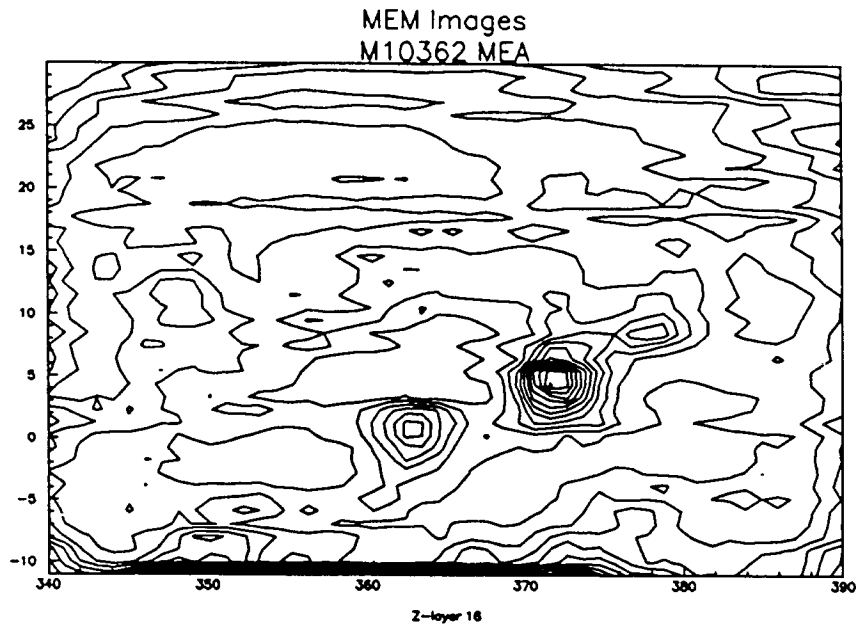


Fig 3.3. Increasing the background to 16 times the counts from a single source reduces the source visibility significantly.

various positions were occulted by a lead shield which was not completely efficient; therefore there is real structure present in the background, and the extra features are at least in part due to this structure. Pure 'room background' data would have been preferable for this test but not enough of this is available. The effect of undefined parts of the image is even more noticeable here.

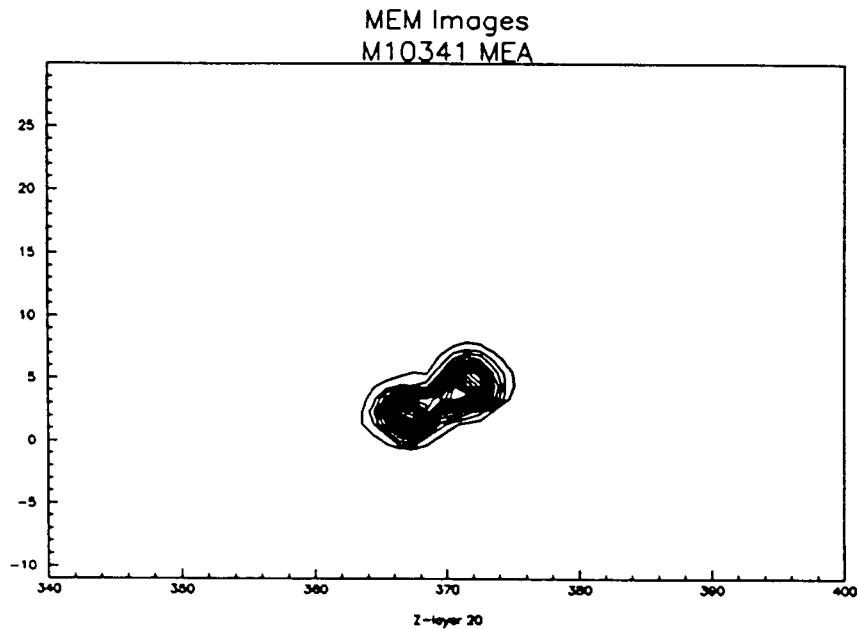


Fig 3.4. Two sources separated by 5° are resolved; the intrinsic source diameter of 2° contributes to the overlap, so the true resolution is better than apparent here.

A test of the angular resolution is shown in Fig 3.4, where two sources separated by 5° are used. The sources are clearly resolved, but there is significant fill-in between the sources; the intrinsic angular width (2°) due to source proximity (see above) contributes to this, as does the bin size used, 1° in (λ, ψ) and 2° in $\bar{\varphi}$ which is really too large fully to exploit the PSF. Considering both these effects the source resolution for strong sources is probably $2-3^\circ$.

All of these tests were made with just one D1 module to avoid source spreading; this also has the effect of reducing the coverage of the geometrical response g in Equation 1. In flight all D1 modules can be used (sources at infinity) and the geometrical response is in this case more uniform.

One problem which always arises in MEM applications is when to stop the iteration process, i.e. which of the images is the 'best' one? In principle we can use the first image which satisfies some statistical test at some confidence level, but in practice the fit may never be acceptable (e.g. by χ^2) due to imperfect knowledge of the instrumental response and also imperfections in the data. The best way to present the results is to show a series of iterations ranging from 'too flat' to 'too structured'. The 'best' map lies somewhere in between and usually it is clear from the series what features are to be trusted. As an example, Fig 3.5 shows the iterations for the case shown earlier in Fig 3.2. The range of images up to 14 are too flat, while images after 22 are breaking up into 'noise'; images between these limits are all acceptable, and indeed they all look much the same.

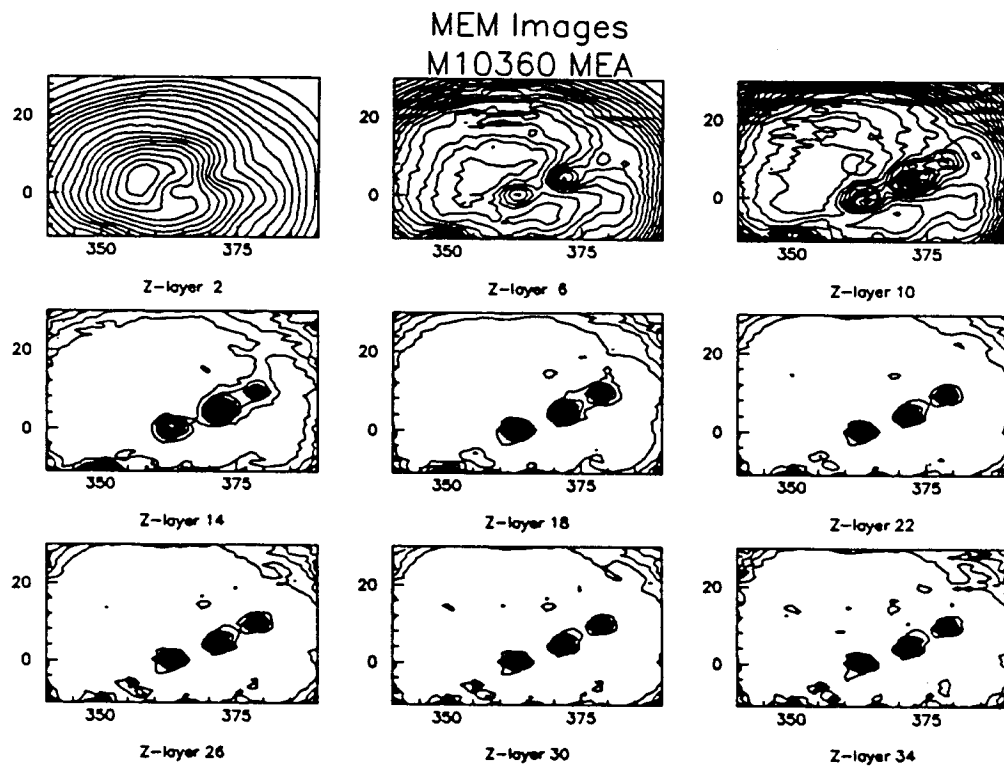


Fig 3.5. Iterations of the maximum entropy algorithm for the same data as Fig 3.2. Starting from a flat map, the fit to the data is improved in each iteration; in the limit the data is overfitted and too much structure appears. The 'best' image lies somewhere between, but presentation of a series of iterations is the best way to indicate the uncertainty in the structure.

4. APPLICATION TO SPECTRAL DECONVOLUTION

One of the scientific objectives of COMPTEL is to study solar flare γ -rays and cosmic γ -ray bursts. The burst detector uses two of the lower (D2) detectors and is described by Winkler et al. (1989). Because the response function contains a significant 'Compton tail' in addition to the photopeak the measured spectrum is significantly modified relative to the input spectrum; deconvolution is therefore very desirable particularly for spectra showing absorption/and or emission lines. The alternative method is to fit an explicit model to the data; but a 'hypothesis free' method is always useful in order to suggest what should be included in the model.

Cabeza-Orcel. et al (1989) have studied the application of the MEM COMPTEL burst data and SMM solar flare data. They used calibration data from Ba^{133} (0.356 MeV), Na^{22} (0.511 MeV annihilation line) and Cs^{137} (0.662 MeV) sources together with a provisional response matrix. In one test the data were added to simulate a multi-peak spectrum and an appropriate background estimate based on a background run was subtracted; the result is shown in Fig 4.1.

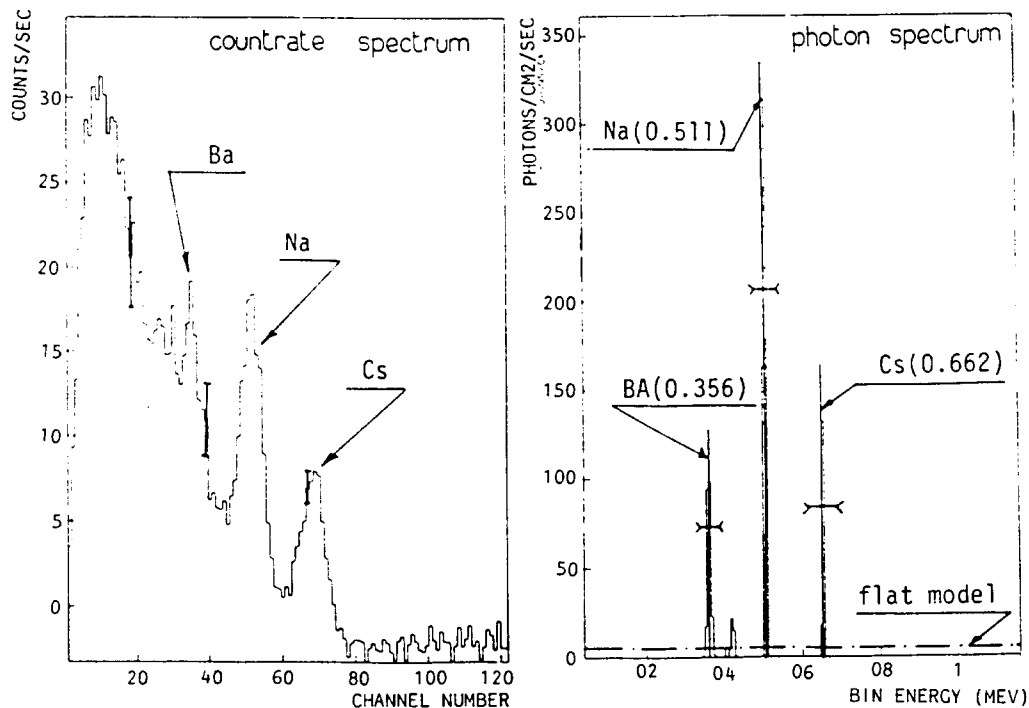


Fig 4.1. MEM deconvolution of a combination of calibration sources

The results of several tests indicated that the source spectrum is correctly recovered as long as the signal/background is at least 10% corresponding to an incident flux of a few 10^{-5} ergs/cm²/sec, and the noise is no more than 35% of the background-subtracted signal amplitude. The lines were correctly placed to within 1% and the full width at half maximum never exceeds the detector resolution. Below this flux however the method was found much less successful.

Cabeza-Orcel. et al (1989) also used solar flare data from the Solar Maximum Mission Gamma-Ray Spectrometer (SMM GRS); the SMM detector is quite similar to COMPTEL burst modules so this provides a realistic test on data of astrophysical interest. The response matrix consists of 476*500 elements. The data used were for the famous solar flare event

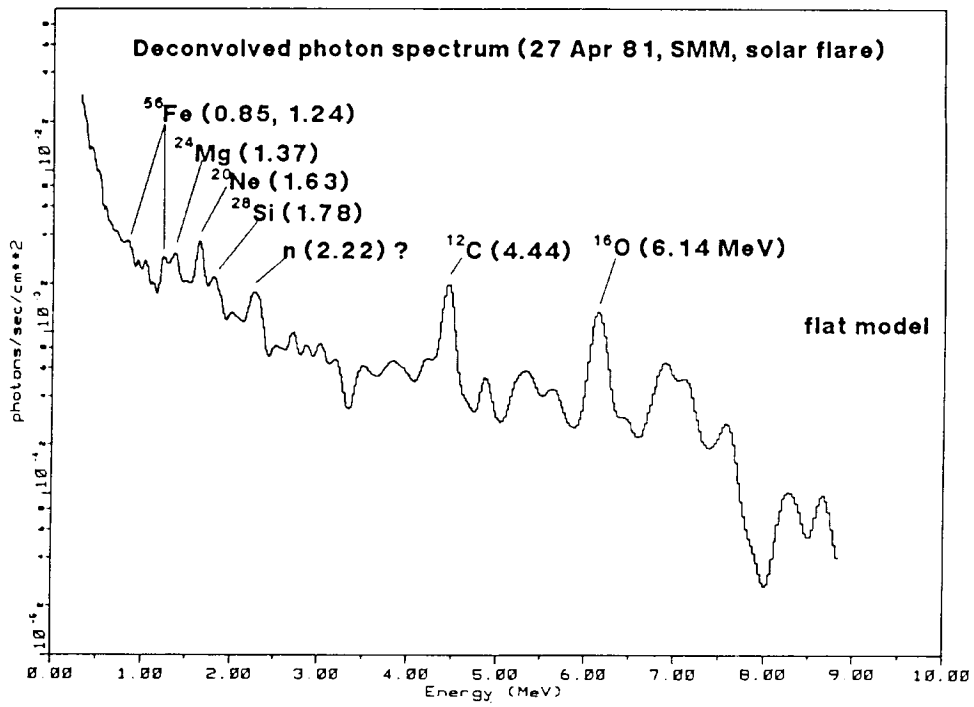
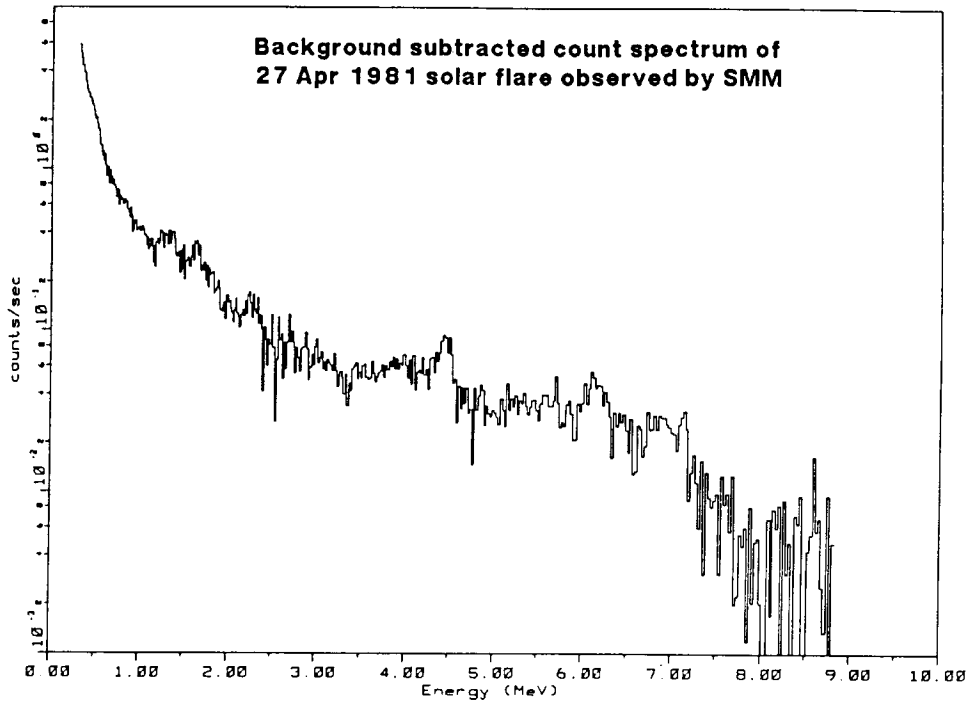


Fig 4.2: SMM solar flare data and MEM deconvolution

of 27th April 1981 (1722 sec duration). The deconvolution (Fig 4.2) shows most of the lines expected in a specific model (Murphy et al. 1985), with the exception of the e^+e^- annihilation line.

The method has been adopted as the standard deconvolution technique for COMPTEL burst data. At present the MEMSYS2 package has been used, but in future it is hoped to take advantage of recent (Bayesian) enhancements of MEMSYS which allow (for example) error estimates on spectral features to be obtained in addition to simply the deconvolution itself.

5. CONCLUSIONS

Maximum entropy promises to be an important component of COMPTEL data analysis, both in the skymapping and spectral deconvolution areas. There is no doubt that much experience will have to be accumulated on in-flight data before the method is optimized, but the calibration data have provided an excellent basis for evaluating the practicability of the method with the real instrument response, and getting the software into a form where it can address real data.

REFERENCES

- Cabeza-Orcel P, Bennett K, Winkler C, (1989),
Proc. GRO Science Workshop , NASA/GSFC, 4-512
Diehl R, Strong A W , (1987), Data Analysis in Astronomy III , Plenum, New York, 55
Gull S F , Skilling J , (1984), IEE Proceedings , 131, 646-659
Murphy R et al., (1985), Proc. 19th Cosmic Ray Conf. , 4 , 249
Skilling J, Strong A W, Bennett K, (1979), Mon. Not. R. astr. Soc., 187, 145-152
Strong A W et al., (1990), Proc. 21st Int. Cosmic Ray Conf. , 4 , 154
Varendorff M, (1991), Thesis, TU München
Winkler C et al., (1989), Proc. GRO Science Workshop , NASA/GSFC , 4-470